Algal Research 12 (2015) 350–358

Contents lists available at ScienceDirect

Algal Research

journal homepage: www.elsevier.com/locate/algal

Review

New mechanistic model to simulate microalgae growth

Alessandro Solimeno [a], Roger Samsó [a], Enrica Uggetti [a], Bruno Sialve [b], Jean-Philippe Steyer [b], Adrián Gabarró [a], Joan García [a,*]

[a] GEMMA — Group of Environmental Engineering and Microbiology, Department of Hydraulic, Maritime and Environmental Engineering, Universitat Politècnica de Catalunya-BarcelonaTech, c/Jordi Girona, 1-3, Building D1, E-08034 Barcelona, Spain
[b] INRA, UR0050, Laboratoire de Biotechnologie de l'Environnement, Avenue des Etangs, Narbonne F-11100, France

ARTICLE INFO

Article history:
Received 9 April 2015
Received in revised form 10 September 2015
Accepted 11 September 2015
Available online 6 October 2015

Keywords:
Photobioreactors
$HRAP_S$
Photolimitation
Oxygen inhibition
Irradiance
Photosynthetic factories

ABSTRACT

The prospect of treating wastewater and at the same time producing microalgae biomass is receiving increasing attention. Mechanistic models for microalgae growth in wastewater are currently being developed for new systems design as well as to improve the understanding of the involved biokinetic processes. However, mathematical models able to describe the complexity of microalgal cultures are still not a common practice. The aim of the present study is to present and calibrate a new mechanistic model built in COMSOL Multiphysics™ platform for the description of microalgae growth. Carbon-limited algal growth, transfer of gases to the atmosphere; and photorespiration, photosynthesis kinetics and photoinhibition are included. The model considers the growth of microalgae as a function of light intensity and temperature, as well as availability of nitrogen and other nutrients. The model was calibrated using experimental data from a case study based on the cultivation of microalgae species in synthetic culture medium. The model was able to reproduce experimental data. Simulation results show the potential of the model to predict microalgae growth and production, nutrient uptake, and the influence of temperature, light intensity and pH on biokinetic processes of microalgae.

Contents

* Corresponding author.
E-mail address: joan.garcia@upc.edu (J. García).

http://dx.doi.org/10.1016/j.algal.2015.09.008
2211-9264/

1. Introduction

Microalgae are nowadays used to produce a variety of compounds of interest for different industrial sectors such as aquaculture and animal feed, human nutrition, cosmetics and nutraceutics as well as pharmaceutics [1,55]. In addition, these microorganisms have a great potential for CO_2 capture and biofuels production such as biodiesel [16]. In fact, in recent years a tremendous effort has been made in numerous research centres to obtain biodiesel from microalgae; however the industrial production of biodiesel is still far from becoming a consolidated technology [11,15].

Another biotechnological application of microalgae is their use for wastewater treatment. Since the late 1950s, the growth of mixed consortia of microalgae and bacteria has been promoted in high rate algal ponds (HRAP) with that aim [40]. In these treatment systems microalgae provide the required oxygen for the degradation of certain wastewater constituents by aerobic bacteria. Though the interest in this technology decreased over the years, in the current context of energy crisis it is skyrocketing again due to its dual benefit: treating wastewater and producing algal biomass that can be valorised in the form of biofuels or bioproducts [47].

All these microalgal biotechnology applications require tools that allow us to forecast biomass production in order to ensure feasibility for valorisation of microalgae as products or biofuels [6]. At the same time production forecasting is challenging because microalgae growth depends on many parameters such as solar radiation, nutrients availability (e.g. carbon and nitrogen) as well as on certain inhibitory conditions (e.g. excess of oxygen in the algal culture).

Mathematical models offer a great opportunity to study the simultaneous effect of different factors affecting algal growth and allow forecasting algal production. Research on microalgae growth kinetics modelling started with the pioneering work by Droop [20,21]. Since then a number of researchers have developed models based on single factors such as light intensity [30], temperature [24], nitrogen [7] and photosynthesis and photoinhibition effects [58]. In fact, there is a vast array of models that predict biomass production as a function of light intensity [59]. This results from the fact that light cannot be easily controlled at full-scale microalgae cultures, in contrast to other factors which are maintained at optimal conditions to avoid limiting or inhibitory effects (e.g. pH, nutrients and mixing conditions). Recently, models of increasing complexity with two or more factors have been developed [9,45]. As an example, in the model by Bernard [7] light intensity and nitrogen are the limiting factors for microalgae growth. Most of these previous models use few parameters to describe the inherent complexity of algal cultures, especially so in the particular case of microalgae grown in wastewaters, where carbon and nitrogen limitations can be significant. Therefore the main objective of this paper is to present a new mechanistic model that includes crucial physical and biokinetic processes for the description of microalgae growth in different types of cultures, and most particularly in wastewater.

The main source of inspiration for building the presented model was the River Water Quality Model 1 (RWQM1) of the International Water Association [49]. RWQM1 was selected because it belongs to a family of widely accepted models (e.g. the Activated Sludge Models (ASM)) which share the same presentation, notation and structure for compounds, processes, and kinetic constants [29,50]. Moreover, RWQM1 is unique in the IWA family models because it considers microalgae activity.

The model was implemented in the COMSOL Multiphysics™ software, which solves differential equations using the finite elements method (FEM). For calibration we used experimental data obtained from a culture medium simulating treated urban wastewater (i.e. secondary effluent). This model will provide new insight into the functioning of microalgae cultures, and will help to explore the simultaneous effects of factors affecting microalgae growth. It is also a part of a more ambitious project through which we intend to develop a complete model to simulate mixed cultures of microalgae and bacteria treating wastewater (like HRAP or photobioreactors).

2. Model description

2.1. Conceptual model

The conceptual understanding that we have of the modelled system is shown in Fig. 1. This figure shows that microalgae grow with light, consume substrates (i.e. carbon and nitrogen) and release oxygen. Note that other nutrients (e.g. phosphorus) and micronutrients are not considered to be limiting factors because they are usually highly available in wastewater (which is the type of culture that mainly addresses the present model) [35]. As a result of microalgal activity, hydroxide ions concentration and pH increase. Increasing pHs displace the equilibrium of the carbon species towards the formation of carbonates. In darkness, endogenous respiration and inactivation of microalgae release carbon dioxide, the concentration of hydrogen ions increases and pH decreases. By decreasing pH the carbon equilibrium shifts and carbonate turns into bicarbonate, which can be used as substrate again in the presence of light.

2.2. Model components

The model follows the most commonly used nomenclature in the IWA models and considers 10 components. From these components, there are 9 dissolved components and one particulate component corresponding to microalgae biomass (X_{ALG}).

2.2.1. Dissolved components

1. S_{NH4} [gNH_4^+-N m^{-3}]: *Ammonium nitrogen*. Nitrogen present in the water as ammonium. It is produced through the processes of endogenous respiration and through inactivation of microalgae. It is consumed through the growth of microalgae.
2. S_{NH3} [gNH_3-N m^{-3}]: *Ammonia nitrogen.* Nitrogen in the form of ammonia. It is in chemical equilibrium with ammonium (S_{NH4}). Its concentration decreases by volatilization to the atmosphere.
3. S_{NO3} [gNO_3^--N m^{-3}]: *Nitrate nitrogen.* Nitrogen available as nitrate. It is consumed by microalgae (X_{ALG}).
4. S_{O2} [gO_2 m^{-3}]: *Dissolved oxygen.* Concentration of dissolved oxygen in the water. It is produced by the growth of microalgae due to

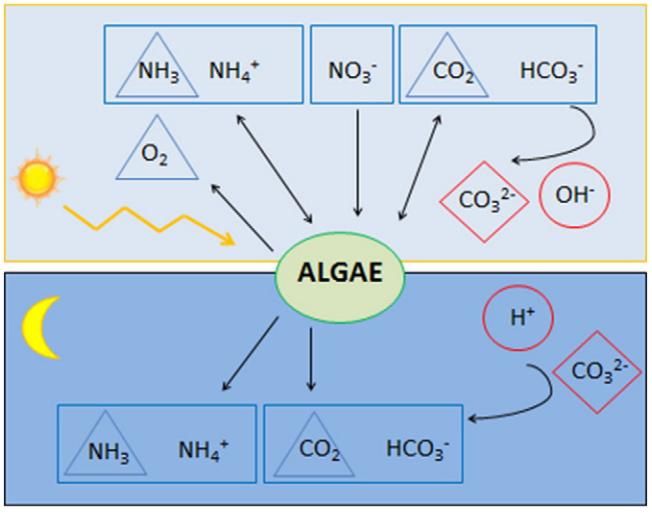

Fig. 1. General schematic representation of the conceptual model. Microalgae (green ellipse), substrates (rectangles), gaseous species (triangles) and species depending on algal activity which are neither substrates nor gases (diamonds and circles). Other nutrients (e.g. phosphorus) and micronutrients are not limiting factors.

photosynthesis and consumed during the processes of endogenous respiration and inactivation of microalgae. It can also be transferred to the atmosphere.

5. S_{CO2} [gCO_2-C m^{-3}]: *Carbon dioxide*. Carbon as carbon dioxide. It is consumed by microalgae and is produced through the processes of endogenous respiration and inactivation. Moreover, it is in chemical equilibrium with bicarbonate (S_{HCO3}) and carbonate (S_{CO3}), and like dissolved oxygen (S_{O2}), it can be transferred to the atmosphere.
6. S_{HCO3} [$gHCO_3^-$-C m^{-3}]: *Bicarbonate*. Carbon as bicarbonate. It is in chemical equilibrium with carbon dioxide (S_{CO2}) and carbonate (S_{CO3}). It is consumed by microalgae.
7. S_{CO3} [gCO_3^{2-}-C m^{-3}]: *Carbonate*. Carbon in the form of dissolved carbonate. It is in chemical equilibrium with bicarbonate (S_{HCO3}) and carbon dioxide (S_{CO2}). Carbonate is not used by microalgae as carbon source.
8. S_H [gH m^{-3}]: *Hydrogen ions*. Concentration of hydrogen ions in the water. They are involved in carbon and ammonium equilibrium systems. The concentration of hydrogen ions decreases with the growth of microalgae and increases with endogenous respiration and inactivation.
9. S_{OH} [gOH^--H m^{-3}]: *Hydroxide ions*. Concentration of hydroxide ions in the water. They are in equilibrium with hydrogen ions.

2.2.2. Particulate components

10. $\mathbf{X_{ALG}}$ [gCOD m^{-3}]: *Microalgae biomass*. Concentration of microalgae. It increases with growth processes and decreases by endogenous respiration and inactivation.

Note that it is expressed in gCOD (chemical oxygen demand) m^{-3} as it is a common practice to express organic matter concentrations in all IWA models. Microalgae biomass is transformed from COD to TSS (total suspended solids) assuming a ratio COD $TSS^{-1} = 0.80$ [31,54].

2.3. Processes

Table 1 shows a list of the processes included in the model and the equations describing their rates. Table 2 shows the matrix of stoichiometric parameters.

2.3.1. Algal processes

- *Growth of microalgae* (processes 1a and 1b in Table 1). The increase of microalgae biomass per unit of time (growth rate) is expressed as the product of their maximum specific growth rate (μ_{ALG}) by their concentration at that point in time (X_{ALG}) and by corrective factors (in the form of Monod functions) [40] that limit or inhibit their growth.

Microalgae grow with both carbon dioxide (S_{CO2}) and bicarbonate (S_{HCO3}). Note that in the matrix of stoichiometric parameters (Table 2) only the reaction rate of carbon dioxide is affected by microalgae growth because the concentration of bicarbonate is already in chemical equilibrium with it. Carbon dioxide (S_{CO2}) inhibits microalgae growth at very high concentrations based on the results of Silva and Pirt [53]. More precisely, it has been observed that in closed photobioreactors CO_2 behaves as an inhibitor at partial pressures above 0.6 atm, which is equivalent to a dissolved CO_2 concentration of 440 mg CO_2 L^{-1} at 37 °C [53]. Inhibition caused by CO_2 is due to the compound itself as well as its effect on acidity, which in the current status of the model cannot be distinguished. Microalgae grow with ammonia and ammonium (S_{NH4}–S_{NH3}) or with nitrate (S_{NO3}) as nitrogen source. When ammonium (or ammonia, note that they are in chemical equilibrium) and nitrate are both present, ammonium is generally preferred [42,52,56]. To represent this phenomenon, the highlighted term that describes the inhibiting effect of ammonia and ammonium on growth of microalgae once nitrate has been introduced in Eq. (1) (process 1b in Table 1).

$$\rho_{1b} = \mu_{ALG} * f_{T,FS}(T) * \eta_{PS}(I, S_{O2}) * \frac{S_{CO2} + S_{HCO3}}{K_{C,ALG} + S_{CO2} + S_{HCO3} + \frac{S_{CO2}^2}{I_{CO2,ALG}}} * \frac{S_{NO3}}{K_S + S_{NO3}} * \frac{K_{N,ALG}}{K_{N,ALG} + S_{NH3} + S_{NH4}} * X_{ALG} \quad (1)$$

Here again note that microalgae growth only affects the reaction rate of ammonia because it is in equilibrium with ammonium (Table 2).

The photosynthetic factor (η_{PS}) takes into account the effects of light intensity (I) and excess of oxygen (S_{O2}) on photosynthesis and therefore on microalgae growth. The following relationship was introduced:

$$\eta_{PS}(I, S_{O2}) = f_L(I) \cdot f_{PR}(S_{O2}) \quad (2)$$

where, f_L is the light factor and f_{PR} the photorespiration factor.

The effects of light intensity on photosynthesis are described by the 'photosynthetic factories' model (PSF) as proposed by Eilers and Peters [23]: at low light irradiance, the rate of photosynthesis is proportional to light intensity because photosynthesis is limited by the rate of capture of photons. When irradiance increases to a certain point, microalgae become 'light saturated' because photosynthesis cannot process more photons. If irradiance increases beyond an inhibitory threshold, the rate of photosynthesis starts to decrease [6,13,18].

In the PSF model it is assumed that microalgae are present in three different states: resting or 'open' (x_1), activated or 'closed' (x_2), and inhibited (x_3) (Fig. 2).

Table 1
Mathematical description of the processes of the model (processes rates).

Processes	Process rate [$M \cdot L^{-3} \cdot T^{-1}$]
1a. Microalgae growth on ammonia	$\rho_{1a} = \mu_{ALG} * f_{T,FS}(T) * \eta_{PS}(I, S_{O2}) * \frac{S_{CO2}+S_{HCO3}}{K_{C,ALG}+S_{CO2}+S_{HCO3}+\frac{S_{CO2}^2}{I_{CO2,ALG}}} * \frac{S_{NH3}+S_{NH4}}{K_{N,ALG}+S_{NH3}+S_{NH4}} * X_{ALG}$
1b. Microalgae growth on nitrate	$\rho_{1b} = \mu_{ALG} * f_{T,FS}(T) * \eta_{PS}(I, S_{O2}) * \frac{S_{CO2}+S_{HCO3}}{K_{C,ALG}+S_{CO2}+S_{HCO3}+\frac{S_{CO2}^2}{I_{CO2,ALG}}} * \frac{S_{NO3}}{K_{N,ALG}+S_{NO3}} * \frac{K_{N,ALG}}{K_{N,ALG}+S_{NH3}+S_{NH4}} * X_{ALG}$
2. Microalgae endogenous respiration	$\rho_2 = k_{resp,ALG} * f_{T,FS}(T) * \frac{S_{O2}}{K_{O2,ALG}+S_{O2}} * X_{ALG}$
3. Microalgae inactivation	$\rho_3 = k_{death,ALG} * f_{T,FS}(T) * X_{ALG}$
4. Chemical equilibrium $CO_2 \leftrightarrow HCO_3^-$	$\rho_4 = k_{eq,1} * (S_{CO2} - \frac{S_H S_{HCO3}}{K_{eq,1}})$
5. Chemical equilibrium $HCO_3^- \leftrightarrow CO_3^{2-}$	$\rho_5 = k_{eq,2} * (S_{HCO3} - \frac{S_H S_{CO3}}{K_{eq,2}})$
6. Chemical equilibrium $NH_4^+ \leftrightarrow NH_3$	$\rho_6 = k_{eq,3} * (S_{NH4} - \frac{S_H S_{NH3}}{K_{eq,3}})$
7. Chemical equilibrium $H^+ \leftrightarrow OH^-$	$\rho_7 = k_{eq,w} * (1 - \frac{S_H S_{OH}}{K_{eq,w}})$
8.Oxygen transfer to the atmosphere	$\rho_{O2} = Ka, O_2 * (S_{O2}^{WAT} - S_{O2})$
9.Carbon dioxide transfer to the atmosphere	$\rho_{O2} = Ka, CO_2 * (S_{CO2}^{WAT} - S_{CO2})$
10. Ammonia transfer to the atmosphere	$\rho_{NH3} = Ka, NH_3 * (S_{NH3}^{WAT} - S_{NH3})$

Table 2
Matrix of stoichiometric parameters that relates processes and components through stoichiometric coefficients in Supplementary Table 3.

State variables → *i* / Processes ↓ *j*		S_{NH4} gN m^{-3}	S_{NH3} gN m^{-3}	S_{NO3} gN m^{-3}	S_{O2} gO_2 m^{-3}	S_{CO2} gC m^{-3}	S_{HCO3} gC m^{-3}	S_{CO3} gC m^{-3}	S_H gH m^{-3}	S_{OH} gH m^{-3}	X_{ALG} gCOD·m^{-3}
1a. Microalgae growth on ammonia	ρ_{1a}	$v_{1,1a}$			$v_{4,1a}$	$v_{5,1a}$			$v_{8,1a}$		$v_{10,1a}$
1b. Microalgae growth on nitrate	ρ_{1b}			$v_{3,1b}$	$v_{4,1b}$	$v_{5,1b}$			$v_{8,1b}$		$v_{10,1b}$
2. Microalgae endogenous respiration	ρ_2	$v_{1,2}$			$v_{4,2}$	$v_{5,2}$			$v_{8,2}$		$v_{10,2}$
3. Microalgae inactivation	ρ_3	$v_{1,3}$			$v_{4,3}$	$v_{5,3}$			$v_{8,3}$		$v_{10,3}$
4. Chemical equilibrium $CO_2 \leftrightarrow HCO_3^-$	ρ_4					$v_{5,4}$	$v_{6,4}$		$v_{8,4}$		
5. Chemical equilibrium $HCO_3^- \leftrightarrow CO_3^{2-}$	ρ_5						$v_{6,5}$	$v_{7,5}$	$v_{8,5}$		
6. Chemical equilibrium $NH_4^+ \leftrightarrow NH_3$	ρ_6	$v_{1,6}$	$v_{2,6}$						$v_{8,6}$		
7. Chemical equilibrium $H^+ \leftrightarrow OH^-$	ρ_7								$v_{8,7}$	$v_{9,7}$	
8. Oxygen transfer to the atmosphere	ρ_{O2}				$v_{4,O2}$						
9. Carbon dioxide transfer to the atmosphere	ρ_{CO2}					$v_{5,CO2}$					
10. Ammonia transfer to the atmosphere	ρ_{NH3}		$v_{2,NH3}$								

Initially microalgae are in open state x_1, ready to capture a photon. When the photon is captured and biochemical reactions start, microalgae turn to activated state x_2. This reaction depends on the rate of activation $\alpha[(\mu E\ m^{-2})^{-1}]$. In activated state microalgae can go back to open state x_1 in dark conditions, or can capture another photon and pass to inhibited state x_3. These two reactions depend on a rate constant of production γ $[s^{-1}]$ and on a rate constant of inhibition β $[(\mu E\ m^{-2})^{-1}]$. Microalgae in the inhibited state turn back to the open state with a rate of recovery δ $[s^{-1}]$.

Considering the principle of mass conservation, the three states can be described by the following system of differential equations (Eqs. (3), (4), (5) and (6)):

$$\frac{dx_1}{dt} = -\alpha \cdot I \cdot x_1 + \gamma \cdot x_2 + \delta \cdot x_3 \tag{3}$$

$$\frac{dx_2}{dt} = \alpha \cdot I \cdot x_1 - \gamma \cdot x_2 - \beta \cdot I \cdot x_2 \tag{4}$$

$$\frac{dx_3}{dt} = \beta \cdot I \cdot x_2 - \delta \cdot x_3 \tag{5}$$

$$x_1 + x_2 + x_3 = 1 \tag{6}$$

When irradiance is not constant, but is a nonlinear function of time (I(t)), this system of differential equations does not have an analytical solution. However, under outdoor conditions, variations of I during the daily solar cycle are very slow with respect to the dynamics of photosynthesis [14,23]. In these conditions x_1 and x_2 are close to equilibrium within less than a second. Therefore it can be assumed that equilibrium is reached instantly, making the left hand side of differential terms equal to zero. Under this assumption, the solution to this system of differential equations is:

$$x_1 = \frac{\gamma\delta + \beta I\delta}{\alpha\beta I^2 + (\alpha+\beta)\delta I + \gamma\delta} \tag{7}$$

$$x_2 = \frac{\alpha\delta I}{\alpha\beta I^2 + (\alpha+\beta)\delta I + \gamma\delta} \tag{8}$$

$$x_3 = \frac{\alpha\beta I^2}{\alpha\beta I^2 + (\alpha+\beta)\delta I + \gamma\delta}. \tag{9}$$

The state in which microalgae can grow is x_2, and therefore in our model the photosynthetic factor is:

$$f_L(I) = x_2 \tag{10}$$

As shown before (Eq. (2)), in microalgae culture photosynthesis not only depends on the solar irradiance, but is also a function of oxygen concentration (for high concentrations). Especially in closed photobioreactors where there is little (if any) oxygen exchange with the atmosphere, the accumulation of this component may inhibit photosynthesis [39]. According to Chisti [15], to prevent such inhibitory effects the dissolved oxygen concentration should never exceed about 400% of air saturation value. The photorespiration factor is introduced in this work to represent this phenomenon in mathematical terms:

$$f_{PR}(S_{O2}) = \begin{cases} 1 - \tanh\left(\dfrac{K_{PR} \cdot \dfrac{S_{O2}}{\tau \cdot S_{O2}^{SAT}}}{1 - \dfrac{S_{O2}}{\tau \cdot S_{O2}^{SAT}}}\right), & S_{O2} \le \tau \cdot S_{O2}^{SAT} \\ 0, \quad S_{O2} > \tau \cdot S_{O2}^{SAT} \end{cases} \tag{11}$$

where S_{O2}^{SAT} $[gO_2\ m^{-3}]$ is the saturation concentration of oxygen in the air. The photorespiration inhibition constant (K_{PR}) and the coefficient of excess dissolved oxygen (τ) are parameters that have to be calibrated during the application of the model.

The effect of photorespiration does not affect microalgal production if the concentration of oxygen in water is clearly lower than τ times the saturation concentration, as is the case of open photobioreactors [15]. However, when the concentration of oxygen tends towards saturation (τS_{O2}^{SAT}) the photorespiration factor decreases, hindering microalgae growth.

The thermic photosynthetic factor ($f_{T,FS}$) takes into account the effects of temperature on microalgae growth and also on endogenous respiration and inactivation processes (1a, 1b, 2 and 3 in Table 1, respectively). Water temperature varies on both diurnal and seasonal scales, affecting both microalgal photosynthesis and respiration rates. The optimal temperature for algal growth ranges between 15 °C and 25 °C,

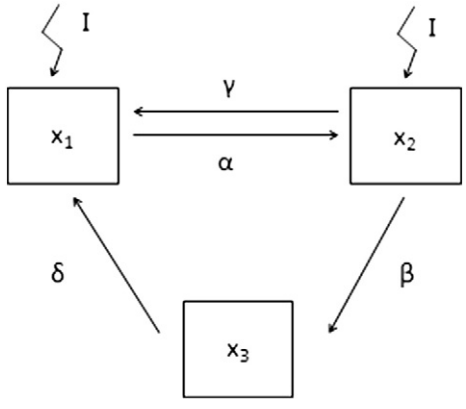

Fig. 2. Three different states and relationships of the photosynthetic factories model (PSF): open (x_1), closed (x_2) and inhibited (x_3) (adapted from Eilers and Peeters [23]).

depending on the species [8,35]. The thermic photosynthetic factor is represented in the model following the work of Dauta et al. [19]:

$$f_{T,FS}(T) = e^{-\left(\frac{T-Topt}{s}\right)^2} \quad (12)$$

where T_{opt} was assumed equal to 25 °C [19] and *s* is a parameter value for empirical fitting.

- *Endogenous respiration* (process 2 in Table 1). The rate of this process is expressed as the product between the maximum rate of endogenous respiration ($k_{resp,alg}$), the concentration of microalgae, the thermic photosynthetic factor (the same as used for the growth of microalgae) and Monod function relates limiting oxygen concentration to a microalgae growth rate.
- *Inactivation of microalgae* (process 3 in Table 1). The rate of this process is expressed as the product of the maximum rate of inactivation ($k_{death,alg}$) by the concentration of microalgae and by thermic photosynthetic factor (the same as for growth) [49].

2.3.2. Chemical equilibrium reactions

Chemical equilibria affect carbon, nitrogen and the balance of hydrogen and hydroxide ions (processes 4, 5, 6 and 7 in Table 1). The rates of these chemical reactions (ρ_i) [g m^{-3} d^{-1}] are obtained with the following general equation [5]:

$$\rho_i = Keq,i\,(S_i - S_{eq,i}) \quad (13)$$

Where i = 1…n and n is the number of chemical species in equilibrium, $k_{eq,i}$ [d^{-1}] is the dissociation constant of reaction i, S_i [g m^{-3}] is the concentration of the i^{th} component and $S_{eq,i}$ [g m^{-3}] is the concentration at equilibrium.

2.3.3. Transfer of gases to the atmosphere

Transfer rates of oxygen, carbon dioxide and ammonia between water and the atmosphere (processes 8, 9 and 10 in Table 1) are given by the general equation [5]:

$$\rho_j = Ka,j\left(S_j^{WAT} - S_j\right) \quad (14)$$

where j = 1…m and m is the number of transfer rates, S_j^{WAT} [g m^{-3}] is the saturation concentration of j^{th} gas in the water, S_j [g m^{-3}] is the gas concentration in the water and $K_{a,j}$ is the overall mass transfer coefficient of j^{th} gas [d^{-1}]. K_a depends on the temperature, the nature of the gas and the liquid and the extension of the surface interface.

2.4. Effects of temperature, irradiance and pH

Temperature, irradiance and pH also affect the rates the processes described previously.

Irradiance (**I**(λ)) [μE (m^2 s)$^{-1}$]: wavelength-specific *irradiance or light intensity*. It is also known in literature as a photon flux density (PFD).

In the present model irradiance was expressed as photosynthetically active radiation (PAR), which includes wavelengths between 400 and 700 nm [60]:

$$PAR = \int_{400\ nm}^{700\ nm} I(\lambda)d\lambda \quad (15)$$

If measured PAR values are not available, estimated values at any Earth geographical location can be calculated from coordinates with the equations presented in Table 3 [3].

Water temperature (**T** [°C]): *water temperature*. Microalgae processes are influenced by temperature described by thermic photosynthetic factor Eq. (12).

Table 3
Initial concentrations of the components in the mesocosms.

Component	Concentration	Units
Dissolved Components		
S_{NH4}	8.1	gN-NH_4 m^{-3}
S_{NH3}	0.685	gN-NH_3 m^{-3}
S_{NO3}	11.37	gN-NO_3 m^{-3}
S_{CO2}	0.8	gC-CO_2 m^{-3}
S_{HCO3}	100	gC-HCO_3 m^{-3}
S_{CO3}	1.17	gC-CO_3 m^{-3}
S_{O2}	8	gO_2 m^{-3}
S_H	$3.16 * 10^{-6}$	gH m^{-3}
S_{OH}	$2.83 * 10^{-3}$	gH-OH m^{-3}
Particulate Component		
X_{ALG}	100	gTSS m^{-3}

pH [−]. pH of the aqueous medium is obtained from hydrogen ions concentration (S_H). pH value displaces the equilibrium of the carbon and nitrogen species.

2.5. Stoichiometry and parameter values

The stoichiometric matrix is presented in Table 2 and is based on the structure of IWA models (Petersen matrix). Values of biokinetic, physical and chemical parameters are shown in Supplementary Tables 1–2. Mathematical expressions of the stoichiometric coefficients of each process are shown in Supplementary Tables 3–4.

Using Tables 1 and 2, the reaction rate for each component of the model (r_i) is obtained with:

$$r_i = \sum\nolimits_j v_{j,i} * \rho_j \quad (16)$$

where i is the number of components and j is the number of processes; ρ_j is the reaction rate for each process j and $v_{i,j}$ is the stoichiometric coefficient. The expressions of stoichiometric coefficients related to microalgae processes are based on the fractions of carbon ($i_{C,ALG}$), hydrogen ($i_{H,ALG}$), oxygen ($i_{O,ALG}$) and nitrogen ($i_{N,ALG}$) (Appendix, Supplementary Tables 3–4).

3. Experimental verification

Experiments were carried out in a batch mesocosm microalgae culture located outdoors at the facilities of the Laboratory of Environmental Biotechnology (LBE, INRA) in Narbonne, South of France (43°11′N, 3°00′E, 13 m A.M.S.L.). The mesocosm consisted of a cylindrical PVC container with a surface area of 1.30 m^2 and a depth of 0.55 m (nominal volume 500 L). A drainage pump ensured continuous stirring of culture medium.

Experiments started on January 23rd 2012. The mesocosm (without replicates) was manually filled with 450 L of medium. 50 L of inoculum with the microalgae *Scenedemus* sp. were added. The medium was prepared as to simulate the mineral composition of a wastewater. A commercial mineral fertilizer (Antys8, Frayssinet, France) (80 g L^{-1} TN, 50 g L^{-1} P_2O_5) was diluted into tap water (0.16/1000), and 0.03 g L^{-1} of NH_4Cl were added to increase nitrogen concentration. The experiments lasted 9 days, and no new fresh medium was added during the entire experimental period.

Photosynthetically active radiation (PAR) was measured with a probe (Sky Instruments PAR Quantum Sensor) located on the surface of mesocosms; data were recorded every 5 min. Water temperature and pH were measured with pH and temperature probes (InPro 426i, Mettler Toledo, CH) every morning. During the 9 days water temperature varied between 9 and 18.7 °C (January and February are the coldest months in the region) and the light intensity (PAR) ranged from 3.25 and 655 μE m^{-2}·s.

Samples of the microalgae culture were taken after 2, 4, 8 and 9 days, and analysed for total suspended solids (TSS) as indicator of algal biomass and ammonium (NH_4^+-N) according to conventional procedures indicated in the standard methods [2].

4. Model implementation and calibration procedure

The model described in Section 2 was implemented in COMSOL Multiphysics™ v4.3b software. A 0D domain was used to represent the experimental reactor (mesocosms), which can be considered in perfect mixing, and therefore transport of aqueous phase species (i.e. dissolved and particulate) can be ignored.

The model was calibrated using available data for the 9 days of experimentation. Manual trial and error adjustment of parameters was used to match measured data as much as possible using graphical representations.

The concentrations of components in the mesocosms measured at the beginning of the experiment are shown in Table 3.

From the 31 parameters implemented in the model, 16 parameters were obtained from the existing River Water Quality Model [49]. Those parameters related to transfer of gases to the atmosphere, temperature, photorespiration and carbon limitation on microalgae growth are not included into the RWQM1 and they were obtained from other literature cited in Tables. Morris's uncertainty method [41] was applied to screening which parameters had a greater influence on the simulation response. Based on a previous uncertainty analysis, the model was calibrated by adjusting the values of the maximum growth rate of microalgae (μ_{ALG}), the transfer of gases to the atmosphere and the photorespiration inhibition constant (K_{PR}). Calibration was conducted by comparing simulated and experimental data curves.

5. Results

Biomass concentration in the mesocosm increased from 100 gTSS m^{-3} at the beginning of the experiment to around 210 gTSS m^{-3} after 9 days. Fig. 3 shows that the model was able to reproduce such growth pattern with an acceptable accuracy. Interestingly, the simulated curve has a wavelike trend which indicates that the model is able to reproduce microalgae growth (crests) and inactivation (trough) cycles occurring during daytime and at night, respectively.

On the other hand, Fig. 4 shows that pH increased with the growth of microalgae. Despite the fitting between experimental data and simulation results are not as good as in Fig. 3, the model still predicts the general trend shown by the experimentally measured pH values. Again, daily pH variations related to the activity of microalgae can be clearly observed. In darkness, the pH decreases as a consequence of endogenous respiration and inactivation of microalgae which release both carbon dioxide and hydrogen ions, while during the day the pH increases due to photosynthesis.

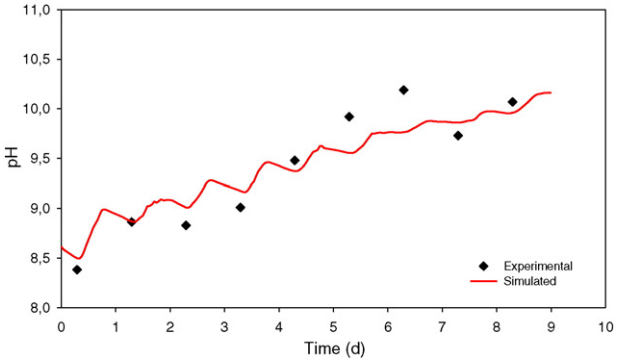

Fig. 4. Experimental (black dots) and simulated (red line) pH values over the 9 days period.

Fig. 5 shows the experimental and simulated ammonium nitrogen concentrations within the mesocosm as well as the simulated nitrate concentration (note that nitrate concentrations were not measured in the experimental study). Once more, the simulated ammonium concentrations match the trend of the experimental measurements with a satisfactory degree of accuracy. Although this phenomenon cannot be demonstrated with the available experimental data, Fig. 5 also shows to what extent microalgae growth used ammonium preferably to nitrate as nitrogen source. After 6 days, the concentrations of S_{NH4} and S_{NH3} were very low but microalgae continued growing, most likely by consuming S_{NO3}. Once again, the daily $S_{NH4} + S_{NH3}$ variations related to the activity of microalgae can be clearly observed.

Fig. 6 shows simulation results for $S_{CO2} + S_{HCO3}$ and S_{CO3} concentrations. $S_{CO2} + S_{HCO3}$ decreased with the growth of microalgae while the concentration of S_{CO3} followed the opposite trend. For increasing values of pH, the equilibrium of the carbon species is displaced towards the formation of carbonates CO_3^{2-}. Daily variations of these carbon species are again related to growth and endogenous respiration and inactivation cycles during daytime and at night, respectively.

The thermic photosynthetic factor ($f_{T,FS}(T)$) which depends exclusively on temperature can range between 0 and 1, where higher values are favourable for algae growth. According to Fig. 7 at the beginning of the experimental study (first 5 days) the conditions were more favourable for microalgae growth, and slightly worsened after that (Fig. 7). Temperature values (shown in Fig. 8, from 9 °C up to 18 °C), give values of the photosynthetic thermal factor oscillating between 0.38 and 0.8. Meanwhile low temperature from day 6 to 9 (from 9 °C

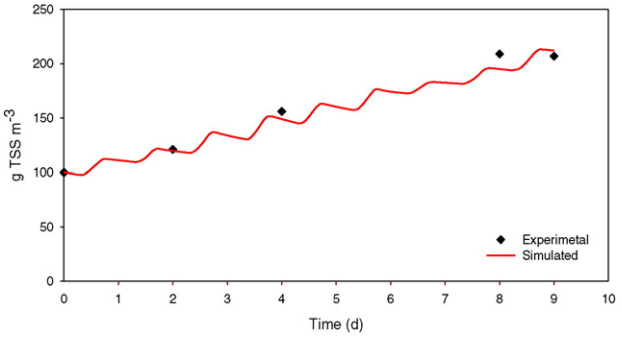

Fig. 3. Experimental (black dots) and simulated (red line) microalgae biomass growth over the 9 days. The crests and troughs of the simulated curve correspond to microalgae growth and inactivation periods during daytime and at night, respectively.

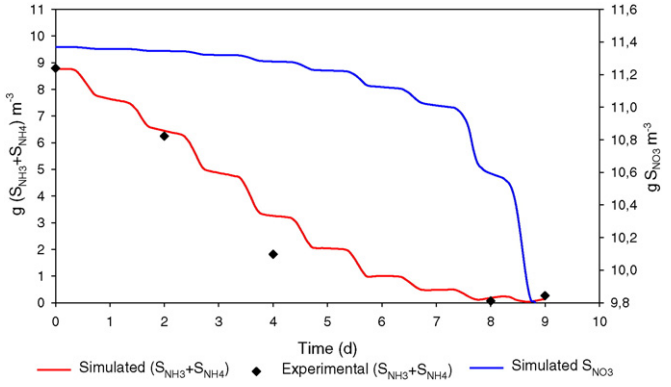

Fig. 5. Comparison between experimental (dots) and simulated (red line) concentrations of ammonium and ammonia and simulated concentrations of nitrate (blue line).

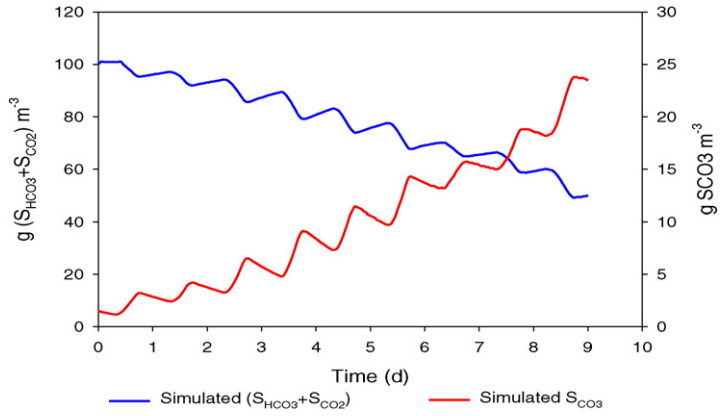

Fig. 6. Microalgae uptake of carbon ($S_{HCO3} + S_{CO2}$) (red line) and S_{CO3} (blue line) simulated curves.

up to 12 °C) decreased microalgae activity. This phenomenon can be observed by looking at the biomass growth rate (slope of the curve of Fig. 3), which decreases slightly after day 5.

Table 4 presents the values of the parameters that were calibrated to obtain the results of Figs. 3 to 7.

6. Discussion

6.1. Innovative features of the model

The main innovation of the current model comes from considering inorganic carbon as a limiting substrate for the growth of microalgae. Previous research on microalgae growth modelling focused on properly describing the dependence of microalgae growth on light, while carbon limitation was not addressed [24,58]. This approach was justified by the fact that the growth of microalgae was studied in photobioreactors in which carbon dioxide was supplied through injection and thus carbon availability was always ensured [8]. However, microalgae grown in wastewater systems such as HRAP, in which no external carbon dioxide is supplied, are usually carbon limited [12]. Hence, in this case, it is essential to consider carbon limitation for a correct estimation of biomass production. In the scenario simulated in this work it was shown how the model was able to simulate the dynamics of the carbon species and in this case it was observed that they did not hinder algae growth. Carbon limitation was implemented in the model by introducing the correction factor $K_{C,ALG}$ in the equation describing the growth rate of microalgae (processes 1a and 1b in Table 1).

On the other hand, excessively high concentrations of carbon dioxide can also be counter-productive and inhibit the growth of microalgae [33]. Although in our experimental setup the excess of carbon dioxide is released to the atmosphere and does not inhibit algae growth, this effect has to be taken into account in closed reactors. To this end, the presented model also implements the inhibitory effect of high concentration of carbon dioxide through the parameter $I_{CO2,ALG}$ [53] (processes 1a and 1b in Table 1).

Temperature has also an effect on the chemical equilibrium of species, pH and gas solubility [10]. In the current scenario, when temperatures decreased, photosynthetic activity also decreased. It is translated into lower pH oscillations (±0.2) during the day/night cycle (Fig. 4).

Photosynthetic processes (e.g. photoinhibition and photolimitation) and photorespiration phenomena were lumped together into a single parameter called the photosynthetic factor $\eta_{PS}(I, S_{O2})$. Among others, the photosynthetic factor includes the influence of irradiance on microalgal growth. In fact, this parameter is considered the main limiting factor in microalgae systems [35,46].

The dynamic model of photosynthesis and photoinhibition presented by Eilers and Peeters [23] solves the system of differential Eqs. (3), (4), (5), and (6) considering constant light intensity (I). In the current work this approach was also adopted. To reproduce the daily variation of light intensity we assume that photosynthetic processes are fast compared to the rate of change of irradiance; hence, the activated photosynthetic factor (x_2) quickly reaches equilibrium with instantaneous irradiance [13]. This simplification was required to obtain the analytical solution of the system of differential Eqs. (3), (4), (5), and (6).

The second term of the Eq. (2) $f_{PR}(S_{O2})$ considers the effects of photorespiration on microalgae growth, a phenomenon so far never modelled in large-scale algal cultures. Chisti [15] imposed a maximum concentration of oxygen dissolved in water equal to four times the value of air saturation. This concentration can be considered equal to

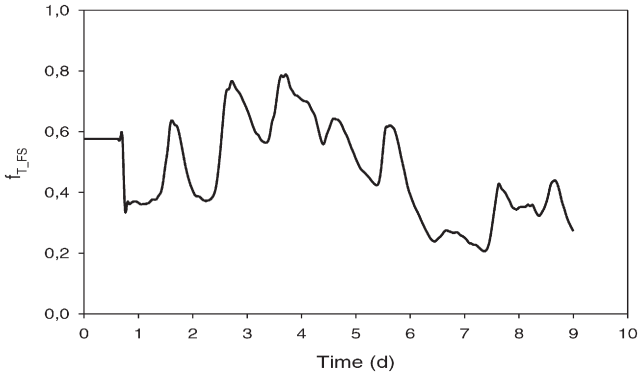

Fig. 7. Evolution of the thermic photosynthetic factor ($f_{T,FS}$) over the 9 days of the experiment.

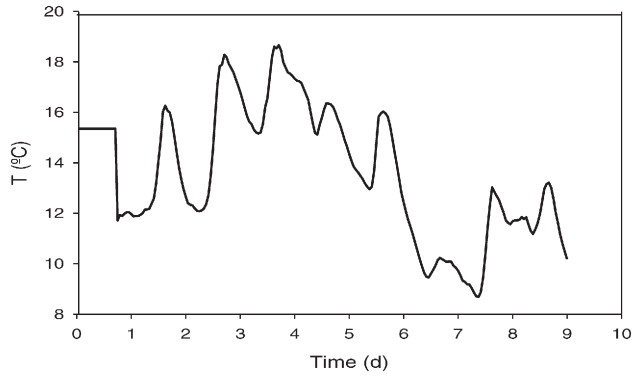

Fig. 8. Temperature measurements (T) over the 9 days of the experiment.

Table 4
Values of calibrated parameters.

Parameter	Description	Value
μ_{ALG}	Maximum specific growth rate of microalgae	1.5 d^{-1}
$K_{a,O2}$	Mass transfer coefficient for oxygen	4 d^{-1}
$K_{a,CO2}$	Mass transfer coefficient for carbon dioxide	0.6 d^{-1}
$K_{a,NH3}$	Mass transfer coefficient for ammonia	0.6 d^{-1}

7.1904 gO_2 m^{-3} [13]. To this restriction must be added the fact that photorespiration phenomenon starts suddenly at high concentration of dissolved oxygen, without significant impact to low concentrations.

Despite the scarce information available on modelling photorespiration, a photorespiration factor $f_{PR}(S_{O2})$ has been proposed in the current work (Eq. (11)), representing the effects of high oxygen concentration in the culture medium. To obtain this expression, the limiting function of the Monod equation was reversed (Fig. 9a). Fig. 9b describes a function that equals zero for negligible dissolved oxygen concentration and increases suddenly with a vertical asymptote when dissolved oxygen concentration reaches the limit saturation (τS_{O2}^{SAT}). The parameter K_{PR}, based on the affinity constant of Monod switching functions, is responsible for the velocity at which the value of the function increases for increasing dissolved oxygen concentrations. The expression that describes the behaviour of photorespiration was obtained by subtracting a unit from the resulting function (Fig. 9c).

In an open reactor oxygen is gradually transferred from the culture medium to the atmosphere, so the effect of photorespiration is negligible (as in our experiment). Photorespiration should be considered in closed photobioreactors.

The calibrated value of the maximum specific growth rate of microalgae (μ_{ALG} = 1.5 [d^{-1}]) fits well within literature ranges [0.4–2 d^{-1}] [49]. Model results proved to be very sensitive to mass transfer coefficients to the atmosphere (Table 4), perhaps because all of these gases participate in a number of processes that either promote or inhibit microalgae growth depending on their concentrations. Indeed, intense photosynthesis can increase daytime dissolved oxygen levels in pond water up to more than 200% of the saturation concentration [26,39]. The exchange of dissolved oxygen between water and the atmosphere occurs rapidly. Thus, to prevent high levels of dissolved oxygen in water, the coefficient of volatilization of oxygen ($K_{a,O2}$) was set so that the oxygen concentration in the culture medium would remain between 9 and 20 gO_2 m^{-3}. Carbon dioxide and nitrogen mass transfer were also calibrated. Although the values of these parameters can be found in the literature as a function of surface interface, in this work we had to calibrate them due to the 0D domain used.

In accordance with daily variation of light intensity, simulated curves show a wavelike trend which indicates that model is able to reproduce the effects related to microalgae processes occurring during daytime and at night.

6.2. Model limitations and future developments

In the current work a 0D domain was used to represent the microalgae culture in the mesocosm. This approach was adequate for the specific characteristics of our experimental system, since we assumed complete mixing conditions. However, HRAP and photobioreactors are characterized by more complex geometries and hydrodynamic regimes. In those cases both flow and transport equations will have to be coupled to the current model to obtain realistic results.

Light attenuation caused by pigments absorption and by the scattering and the shading effect of the microalgae cells themselves was not included in the current version of the model. However, numerous models [48,59] have been developed to estimate the gradient of light taking into account the aspects listed above.

Phosphorous species and their effects on biological processes were not included in this model since this component is usually highly available in wastewaters and hence it does not cause any growth-limiting effects on microalgae [35]. However, predictions on the rate of removal of phosphorous species will require their inclusion in the model, which in fact can be easily done following the approach of the RWQM1.Once all the above mentioned ameliorations are included in the model, it will be capable to predict biomass production in HRAP

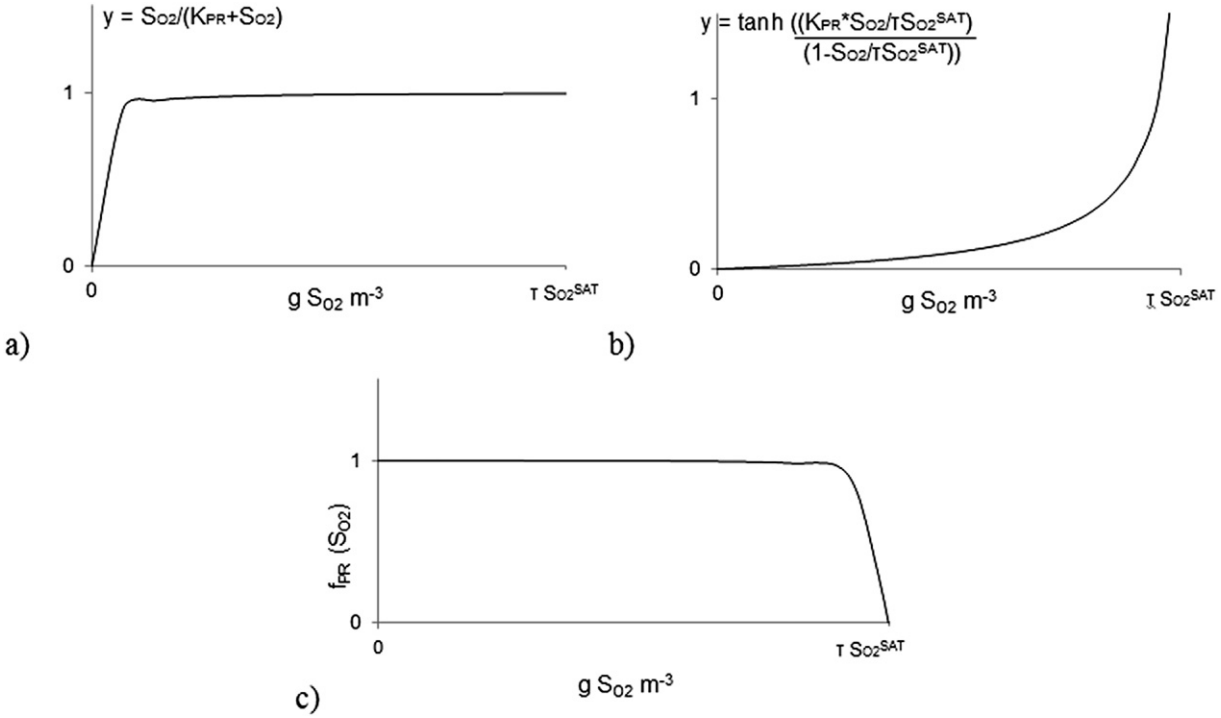

Fig. 9. a) Monod-function for limiting substrate, b) hyperbolic tangent function, and c) photorespiration factor.

and photobioreactors. A following step to fulfil our final objective will be to complete the model with the addition of bacterial processes and to validate the model with other experimental data.

7. Conclusions

In this paper a complex biokinetic model to simulate the dynamics of microalgae growth is presented. The biokinetic model is based on RWQM1 formulation and was implemented in COMSOL Multiphysics™ together with several other processes affecting microalgal biomass production in the widest possible range of microalgal cultures.

The most relevant features of the model is the inclusion an allowance for carbon limitation on the growth of microalgae, as well as the dynamic model of photosynthesis and photolimitation and the description of the effect of photorespiration.

The model was calibrated by comparing simulated results to experimental data on microalgae growth in a mesocosm fed with synthetic culture medium (simulating a secondary effluent) for a period of 9 days. Although the results of the calibration indicate that the model was able to accurately reproduce microalgae growth, changes in nutrient concentrations and pH, the model will require a subsequent verification with larger datasets. The results of this paper have to be considered as a conceptual exercise that could be manually adjusted to fit one single experiment. The value of the exercise is in fact in the development of the equation set and showing that a model based on the set can be run and calibrated to fit a real dataset. Furthermore, the growth of microalgae under natural light/dark cycles and a dynamic model of photosynthesis (PSF) were implemented. The model was able to represent the complex system of photosynthetic growth with simultaneous photoinhibition and photorespiration.

Acknowledgements

We thank Jason Hale for manuscript review. This research was supported by the Spanish Ministry of Economy and Competitiveness through the project DIPROBIO (CTM2012-37860). Alessandro Solimeno also acknowledges the FPU scholarship provided by the Spanish Ministry of Education and Science.

Appendix A. Supplementary data

Supplementary data to this article can be found online at http://dx.doi.org/10.1016/j.algal.2015.09.008.

References

[1] F. Acien, J.M. Fernández Sevilla, E. Molina Grima, Photobioreactors for the production of microalgae, Rev. Environ. Sci. Biotechnol. 12 (2) (2013) 131–151.
[2] APHA-AWWA-WPCF, APHA-AWWA-WPCF Standard Methods for the Examination of Water and Wastewater, twentieth ed. American Public Health Association, Washington DC, 2001.
[3] N.Z. Al-Rawahi, Y.H. Zurigat, N.A. Al-Azri, Prediction of hourly solar radiation on horizontal and inclined surfaces for Muscat/Oma, J. Eng. Res. 8 (2) (2011) 19–31.
[5] D. Batstone, J. Keller, R.I. Angelidaki, S.V. Kalyuzhnyi, S.G. Pavlostathis, A. Rozzi, W.T.M. Sanders, H. Siegrist, V.A. Vavilin, Anaerobic Digestion Model No. 1 (ADM1), IWA Publishing, London, 2002.
[6] Q. Béchet, A. Shilton, B. Guieysse, Modelling the effects of light and temperature on algae growth: state of the art and critical assessment for productivity prediction during outdoor cultivation, Biotechnol. Adv. 31 (2013) 1648–1663.
[7] O. Bernard, P. Masci, A. Sciandra, A Photobioreactor Model in Nitrogen Limited Conditions, Proceedings of the Sixth Conference on Mathematical Modelling, Vienna, 2009.
[8] J.P. Bitog, I.-B. Lee, C.-G. Lee, K.-S. Kim, H.-S. Hwang, S.-W. Hong, I.-H. Seo, K.-S. Kwon, E. Mostafa, Application of computational fluid dynamics for modelling and designing photobioreactors for microalgae production: a review, Comput. Electron. Agric. 76 (2) (2011) 131–147.
[9] J.A. Bonachela, M. Raghib, S.A. Levin, Dynamic model of flexibile phytoplankton nutrient uptake, Proc. Natl. Acad. Sci. U. S. A. 108 (2011) 20633–200638.
[10] R. Bouterfas, M. Belkoura, A. Dauta, Light and temperature effects on the growth rate of three freshwater [2pt] algae isolated from a eutrophic lake, Hydrobiologia 489 (2002) 207–217.
[11] L. Brennan, P. Owende, Biofuels from microalgae—a review of technologies for production, processing, and extractions of biofuels and co-products, Renew. Sust. Energ. Rev. 14 (2) (2010) 557–577.
[12] H.O. Buhr, S.B. Miller, A dynamic model of the high-rate algal bacterial wastewater treatment pond, Water Res. 17 (1983) 29–37.
[13] F. Camacho Rubio, F. García Camacho, J.M. Fernández Sevilla, Y. Chisti, E. Molina Grima, A mechanistic model of photosynthesis in microalgae, Biotechnol. Bioeng. 81 (4) (2003) 459–473.
[14] F. Camacho Rubio, F.G. Acién Fernández, F. García Camacho, J.A. Sánchez Pérez, E. Molina Grima, Prediction of dissolved oxygen and carbon dioxide concentration profiles in tubular photo-bioreactors for microalgal culture, Biotechnol. Bioeng. 62 (1999) 71–86.
[15] Y. Chisti, Biodiesel from microalgae, Biotechnol. Adv. 25 (3) (2007) 294–306.
[16] R.J. Craggs, S. Heubeck, T.J. Lundquist, J.R. Benemann, Algae biofuel from wastewater treatment high rate algal ponds, Water Sci. Technol. 63 (4) (2011) 660–665.
[18] P.A. Crill, The photosynthesis-light curve: a simple analog model, J. Theor. Biol. 6 (1977) 506–516.
[19] A. Dauta, J. Devaux, F. Piquemal, L. Boumnich, Growth rate of four freshwater algae in relation to light and temperatura, Hydrobiologia 207 (1990) 221–226.
[20] M.R. Droop, Vitamin B2 and marine ecology. IV. The kinetics of uptake, growth and inhibition in Monochrysis lutheri, J. Mar. Biol. Assoc. U. K. 48 (1968) 689–733.
[21] M.R. Droop, The nutrient status of algal cells in batch culture, J. Mar. Biol. Assoc. UK 54 (1974) 825–855.
[23] P.H.C. Eilers, J.C.H. Peters, A model for the relationship between light intensity and the rate of photosynthesis in phytoplankton, Ecol. Model. 42 (1988) 199–215.
[24] A. Franz, F. Lehr, C. Posten, G. Schaub, Modeling microalgae cultivation productivities in different geographic locations – estimation method for idealized photobioreactors, Biotechnol. J. 7 (4) (2012) 546–557.
[26] J. García, M. Hernández-Mariné, R. Mujeriego, High rate algal pond operating strategies for urban wastewater nitrogen removal, J. Appl. Phycol. 12 (2008) 331–339.
[29] M. Henze, W. Gujer, T. Mino, M. van Loosdrecht, Activated Sludge Models ASM1, ASM2, ASM2d and ASM3, IWA Scientific and Technical Report No. 9, IWA Publishing, London, UK, 2000.
[30] J. Huisman, Population dynamics of light-limited phytoplankton: microcosm experiments, Ecology 80 (1999) 202–210.
[31] H. Khorsandi, R. Alizadeh, h. Tosinejad, H. Porghaffar, Analysis of nitrogenous and algal oxygen demand in effluent from a system of aerated lagoons followed by polishing pond, Water Sci. Technol. 70 (2014) 1–95.
[33] N. Kurano, S. Miyachi, Selection of microalgal growth model for describing specific growth rate-light response using extended information criterion, J. Biosci. Bioeng. 100 (4) (2005) 403–408.
[35] K. Larsdotter, Wastewater treatment with microalgae—a literature review, Vatten (2006) 31–38.
[39] E. Molina Grima, J. Fernández, G. Acién Fernández, Y. Chisti, Tubolar photobioreactor design for algae cultures, J. Biotechnol. 92 (2001) 113–131.
[40] J. Monod, The growth of bacterial cultures, Annu. Rev. Microbiol. 3 (1949) 371–394.
[41] M.D. Morris, Factorial sampling plans for preliminary computational experiments, Technometrics 33 (2) (1991) 161–174.
[42] E.S. Mostert, J.H. Grobbelaar, The influence of nitrogen and phosphorus on algal growth and quality in outdoor mass algal cultures, Biomass 13 (1987) 219–233.
[45] A. Packer, Y. Li, T. Andersen, Q. Hu, Y. Kuang, M. Sommerfeld, Growth and neutral lipid synthesis in green microalgae: a mathematical model, Bioresour. Technol. 102 (2011) 111–117.
[46] J.B.K. Park, R.J. Craggs, Algal production in wastewater treatment high rate algal ponds for potential biofuel use, Water Sci. Technol. 63 (10) (2011) 2403–2410.
[47] J.B.K. Park, R.J. Craggs, A.N. Shilton, Wastewater treatment high rate algal ponds for biofuel production, Bioresour. Technol. 102 (1) (2011) 35–42.
[48] J. Quinn, L. de Winter, T. Bradley, Microalgae bulk growth model with application to industrial scale systems, Bioresour. Technol. 102 (2011) 5083–5092.
[49] P. Reichert, D. Borchardt, M. Henze, W. Rauch, P. Shanahan, L. Somlyódy, P. Vanrolleghem, River water quality model no. 1 (RWQM1): II. Biochemical process equations, Water Sci. Technol. J. Int. Assoc. Water Pollut. Res. 43 (5) (2001) 11–30.
[50] L. Sah, D. Rousseau, C.M. Hooijmans, P. Lens, 3D model for a secondary facultative pond, Ecol. Model. 222 (9) (2011) 1592–1603.
[52] P.J. Syrett, Nitrogen Metabolism of Microalgae, in: T. Platt (Ed.), Physiological Bases of Phytoplankton Ecology, Canadian Bulletin of Fisheries and Aquatic Sciences, 210 1981, pp. 182–210.
[53] H.J. Silva, J. Pirt, Carbon dioxide inhibition of photosynthetic growth of chlorella, J. Gen. Microbiol. 130 (1984) 2833–2838.
[54] M.V. Sperling, Waste Stabilization Ponds, IWA Publishing, London, UK, 2007.
[55] P. Spolaore, C. Joannis-Cassan, E. Duran, A. Isambert, Commercial applications of microalgae, J. Biosci. Bioeng. 101 (2006) 87–96.
[56] W.D.P. Stewart, Algal Physiology and Biochemistry, Blackwell Scientific Publications, Oxford, 1974 (989 pp.).
[58] X. Wu, J. Merchuk, A model integrating fluid dynamics in photosynthesis and photoinhibition processes, Chem. Eng. Sci. 56 (2001) 3527–3538.
[59] S. Yuan, X. Zhou, R. Chen, B. Song, Study on modelling microalgae growth in nitrogen-limited culture system for estimating biomass productivity, Renew. Sust. Energ. Rev. 34 (2014) 525–535.
[60] C. Zonneveld, Light-limited microalgae growth: a comparison of modelling approaches, Ecol. Model. 113 (1998) 41–54.